Biochimica et Biophysica Acta 1798 (2010) 536–543

Contents lists available at ScienceDirect

Biochimica et Biophysica Acta

journal homepage: www.elsevier.com/locate/bbamem

Surface adsorption of protein corona controls the cell internalization mechanism of DC-Chol–DOPE/DNA lipoplexes in serum

Giulio Caracciolo *, Luciano Callipo, Sofia Candeloro De Sanctis, Chiara Cavaliere, Daniela Pozzi, Aldo Laganà

Chemistry Department, 'Sapienza' University of Rome, P.le A. Moro 5, 00185 Rome, Italy

ARTICLE INFO

Article history:
Received 1 September 2009
Received in revised form 15 October 2009
Accepted 9 November 2009
Available online 14 November 2009

Keywords:
Cationic liposome
DNA
Lipoplex
SAXS
Protein corona
Cell transfection

ABSTRACT

Serum has often been reported as a barrier to efficient lipid-mediated transfection. Here we found that the transfection efficiency of DC-Chol–DOPE/DNA lipoplexes increases in serum. To provide insight into the mechanism of lipoplex-serum interaction, several state-of-the-art methodologies have been applied. The nanostructure of DC-Chol–DOPE/DNA lipoplexes was found to be serum-resistant as revealed by high resolution synchrotron small angle X-ray scattering, while dynamic light scattering measurements showed a marked size increase of complexes. The structural stability of DC-Chol–DOPE/DNA lipoplexes was confirmed by electrophoresis on agarose gel demonstrating that plasmid DNA remained well protected by lipids. Proteomics experiments showed that serum proteins competed for the cationic surface of lipid membranes leading to the formation of a rich a 'protein corona'. Combining structural results with proteomics findings, we suggest that such a protein corona can promote large aggregation of intact lipoplexes. According to a recently proposed size-dependent mechanism of lipoplex entry within cells, protein corona-induced formation of large aggregates most likely results in a switch from a clathrin-dependent to caveolae-mediated entry pathway into the cells which is likely to be responsible for the observed transfection efficiency boost. As a consequence, we suggest that surface adsorption of protein corona can have a high biological impact on serum-resistant cationic formulations for in vitro and in vivo lipid-mediated gene delivery applications.

1. Introduction

Nowadays, one of the primary objectives of gene therapy is the development of efficient, non-toxic gene carriers that can effectively deliver foreign genetic material into specific cell types, including cancerous cells [1]. Viral vectors, including retroviruses, adenoviruses and adeno-associated viruses, have a high efficiency of gene delivery, but general concerns about their safety have recently been intensified by a few severe setbacks [2]. This has further increased the interest in nonviral systems that show significantly lower safety risks with respect to viruses, are capable of carrying large molecules and can be produced in large quantities easily and inexpensively. Among non viral gene nanovectors, cationic liposomes (CLs), which are extensively employed as in vitro transfection agents, are emerging as promising candidates for in vivo delivery of nucleic acids for a variety of applications [3,4]. At present, the major disadvantage connected with the use of CL–DNA complexes (lipoplexes) is their unsatisfactorily low efficiency which depends on the poor understanding of their mechanism of transfection, and the chemical and physical parameters of lipoplexes influencing it.

Recent synchrotron X-ray experiments [5–7] have shown that, upon mixing under equilibrium conditions, DNA and CLs self-assemble into novel liquid-crystalline phases of matter among which the so-called multilamellar L_{α}^{C} structure (Fig. 1) is largely the most abundant one. Upon somministration in vivo, lipoplexes might be modified differently by biological fluids before they reach target cells. Understanding of the barrier for in vivo lipofection via different administration routes is, therefore, critical for the development of a suitable gene delivery vector. Among the most difficult barriers to overcome in transfection, serum is well known for its inhibitory effect [8–10]. Over the last few years, several indications have been reported that such an inhibition is largely due to serum proteins that associate with the nanoparticle [10]. Since it is the lipoplex after interaction with serum proteins that is processed by living cells, the study of the interaction of lipoplexes with serum may serve as a fundamental predictive model for the in vivo efficiency of a lipidic vector. Previous physical studies [8–12] showed that on interaction of cationic lipoplexes with serum, a number of undesirable effects may occur ranging from aggregation, ζ-potential neutralization, destabilization of lipoplex structure resulting in DNA release and degradation. However, the precise mechanisms that govern the transfection behaviour of lipoplexes in serum need to be better elucidated.

In the present work, we have investigated the effect of serum proteins on the transfection efficiency (TE) and colloidal stability of 3β-[N-(N′,N′-dimethylaminoethane)-carbamoyl])-cholesterol (DC-Chol)–dioleoylphosphatidylethanolamine (DOPE)/DNA complexes. This system was chosen because it is one of the most efficient and

* Corresponding author. Tel.: +39 06 4991 3076; fax: +39 06 490631.
E-mail address: g.caracciolo@caspur.it (G. Caracciolo).

0005-2736/$ – see front matter © 2009 Elsevier B.V. All rights reserved.
doi:10.1016/j.bbamem.2009.11.007

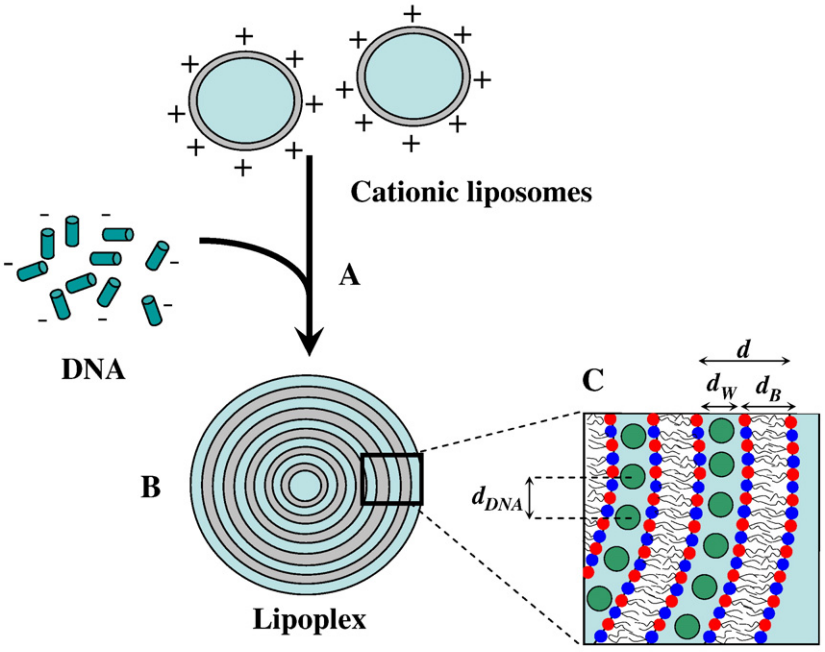

Fig. 1. (A) Mixing of unilamellar cationic liposomes and DNA results in the spontaneous self-assembling of lipoplexes (B) with a multilamellar structure made of alternating lipid bilayers and water layers where DNA is confined. (C) Enlarged view of lipoplex structure showing characteristic distances at the nanoscale (cationic lipids in red, neutral lipids in blue).

widely used non viral formulations in vitro [13,14] and a potentially candidate for in vivo transfection [15]. To this end we have used an integrated approach based on the use of state-of-the-art experimental methodologies: nanostructure of lipoplexes was investigated by synchrotron small angle X-ray scattering (SAXS), size was determined by dynamic light scattering (DLS), DNA-binding ability was evaluated by electrophoresis on agarose gels, while serum proteins associated with the surface of lipoplexes were identified by proteomics experiments.

Here we show that the TE of DC-Chol–DOPE/DNA complexes increases in serum. The nanostructure of complexes is not affected by serum, while negatively charged proteins compete for the cationic membrane surface leading to a 'protein corona' that promotes large aggregation of intact lipoplexes. According to a recently proposed size-dependent mechanism of lipoplex entry within cells [16], we suggest that surface adsorption of protein corona results in a switch from a clathrin-dependent to caveolae-mediated mechanism of internalization responsible for the observed transfection efficiency boost.

2. Materials and methods

2.1. Cationic liposomes preparation

Cationic (3β-[N-(N′,N′-dimethylaminoethane)-carbamoyl])-cholesterol (DC-Chol), and neutral dioleoylphosphatidylethanolamine (DOPE) were purchased from Avanti Polar Lipids (Alabaster, AL) and used without further purification. DC-Chol–DOPE cationic liposomes were prepared according to routinary procedures [17] at a molar fraction of neutral lipid in the bilayer Φ = (neutral lipid/total lipid) (mol/mol) = 0.5. Lipids were dissolved in chloroform and the solvent was evaporated under vacuum for 24 h. The obtained lipid film was hydrated with Tris–HCl buffer solution (10^{-2} M, pH 7.4) to achieve the desired final concentration (10 mg/ml for SAXS experiments, 1 mg/ml for DLS, ζ-potential and electrophoresis experiments). For proteomics experiments the lipid film was hydrated with Tris–HCl (10^{-2} M, pH 7.4), NaCl (0.15 M), and ethylenediaminetetraacetic acid (EDTA; 1 mM) (final concentration 1 mg/ml). The obtained liposome solutions were sonicated to clarity and stored at 30 °C for 48 h to achieve full hydration [17].

2.2. Lipoplexes preparation

For SAXS, DLS, ζ-potential and proteomics measurements, calf thymus (CT) Na-DNA, purchased from Sigma-Aldrich (St. Louis, MO), was used. CT Na-DNA was dissolved in Tris–HCl buffer (5 mg/ml) and was sonicated for 5 min inducing a DNA fragmentation with length distribution between 500 and 1000 bp, which was determined by gel electrophoresis. For transfection and electrophoresis experiments, plasmid DNA (pGL3 which codifies for firefly luciferase), purchased from Promega (Madison, WI), was employed. By mixing adequate amounts of the DNA solutions to suitable volumes of liposome dispersions, self-assembled DC-Chol–DOPE/DNA lipoplexes were obtained. All samples were prepared at a fixed cationic lipid/DNA charge ratio (mol/mol), i.e. ρ = (cationic lipid (by mole)/DNA base) = 3. Such a value was chosen because it corresponds to the middle of a typical plateau region observed for optimal transfection conditions [18,19].

2.3. Cationic liposomes and lipoplexes incubation with serum

After 24 h equilibration, the lipid and lipoplex suspensions were diluted in buffer with fetal bovine serum (FBS, Invitrogen) (50% vol/vol). Diluting FBS with an equal volume of buffer approximates physiological serum concentration [20]. Such samples are indicated in the subsequent text as FBS–CLs and FBS lipoplexes. Storage for 3 days at 4 °C allowed the samples to reach equilibrium [17].

2.4. Cationic liposomes and lipoplexes incubation with human plasma

Human plasma (HP) was prepared as follows. In brief, blood was obtained from Medicina Sprimentale Department (Sapienza

University of Roma) by venipuncture of healthy volunteers (age between 20 and 40), by means of BD™ P100 Blood Collection System (Franklin Lakes, NJ USA) with K_2EDTA anticoagulant and protease inhibitors cocktail. After clot formation, the sample was centrifuged at 1000 RCF for 5 min to pellet the blood cells. The supernatant (plasma) was removed and aliquots stored at −80 °C in labeled tubes. All plasma samples were checked to verify absence of hemolysis. On thawing the plasma was centrifuged again for 2 min at 16 kRCF to further reduce the presence of red and white blood cells. 100 μl of cationic liposomes and lipoplexes suspensions (1 mg/ml) in 10 mM Tris–HCl, pH 7.5, 150 mM NaCl, 1 mM EDTA were incubated with 100 μl plasma on ice. After 1 h, the incubation was conducted to 23 °C for 1 h to promote aggregation. The samples were centrifuged to pellet the particle–protein complexes at 15 kRCF and two centrifugation time were tested (45 and 2 min). The pellet was resuspended in PBS, transferred into a new vial, and centrifuged again to pellet the particle–protein complexes; this procedure was repeated twice. The proteins were eluted from the particles by adding SDS-sample buffer to the pellet and boiling the solution. Then the proteins were separated by 12% SDS/PAGE 1D gels. Afterwards the gels were silver-stained. All experiments were conducted four times to ensure reproducibility of the particle–protein complex pellet sizes, general pattern, and band intensities on the 1D gels.

2.5. Transfection efficiency experiments

Cell lines were cultured in Dulbecco's modified Eagle's medium (DMEM) (Invitrogen, Carlsbad, CA) supplemented with 1% penicillin–streptomycin (Invitrogen) and 10% FBS at 37 °C and 5% CO_2 atmosphere, splitting the cells every 2–4 days to maintain monolayer coverage. For luminescence analysis, mouse fibroblast NIH 3T3 cells were transfected with pGL3 control plasmid. The day before transfection, cells were seeded in 24 well plates (150,000 cells/well) using medium without antibiotics. Cells were incubated until they were 75–80% confluent, which generally took 18 to 24 h. For TE experiments, lipoplexes were prepared by mixing for each well of 24 well plates 0.5 μg of plasmid with 5 μl of sonicated lipid dispersions (1 mg/ml). These complexes were allowed to form for 20 min and lipoplexes were subsequently diluted in buffer or in serum (50% vol/vol) and left for 20 min at room temperature before adding them to the cells. The cells were incubated with lipoplexes in Optimem (Invitrogen) for 6 h to permit transient transfection; the medium was then replaced with DMEM supplemented with FBS. Luciferase expression was analyzed after 48 h and measured with the Luciferase Assay System from Promega, and light output readings were performed on a Berthold AutoLumat luminometer LB-953 (Berthold, Bad Wildbad, Germany). TE was normalized to milligrams of total cellular protein in the lysates using the Bio-Rad Protein Assay Dye Reagent (Bio-Rad, Hercules, CA).

2.6. Synchrotron SAXS measurements

SAXS measurements were carried out at the high-brilliance beamline ID2 at the European Synchrotron Radiation Facility (Grenoble, France). The energy of the incident beam was 12.5 keV ($\lambda = 0.995$ Å), the beam size was 100 μm and the sample-to-detector distance was 1.2 m. The diffraction patterns were collected by a 2D CCD detector (Frelon Camera). We investigated the q range from $q_{min} = 0.04$ Å^{-1} to $q_{max} = 0.5$ Å^{-1} with a resolution of $5 \cdot 10^{-4}$ Å^{-1} (full width at half maximum (FWHM)). The sample was held in a 1 mm-size glass capillary (Hilgenberg, Germany). Measurements were performed at 25 °C. To avoid radiation damage, a maximum exposure time of 3 s/frame was used for any given sample. Satisfactory statistics were obtained by repeating several measurements on fresh samples. The collected 2D powder diffraction spectra were angularly integrated using the *Saxs* package [21]. These data were then corrected for the detector efficiency, empty sample holder and bulk solution.

2.7. Small angle X-ray scattering data analysis

Bragg peak positions, widths and intensities of some diffraction patterns were analyzed by multiple fitting of Lorentzian distributions [22]. Structural parameters of lipid bilayers, i.e. the bilayer thickness, d_B and the water layer thickness, d_W, were calculated by standard procedures, i.e. the electron density profile was deduced from the diffraction data. For further details see the protocols given in [23,24].

2.8. Size and ζ-potential measurements

All sizing and ζ-potential measurements were made on a Zetasizer Nano ZS90 (Malvern, UK) at 25 °C with a scattering angle of 90°. Sizing measurements were made on the neat vesicles dispersions, whereas the samples were diluted 1 in 10 with distilled water for the zeta potential experiments, to obtain reliable and accurate measurements. For all the samples investigated, data show a unimodal distribution and represent the average of at least five different measurements carried out for each sample.

2.9. Agarose gel electrophoresis experiments

Electrophoresis studies were conducted on 1% agarose gels containing ethidium bromide in Tris–borate–EDTA (TBE) buffer. Lipoplexes were prepared by mixing 42 μl of lipid dispersions with 5.4 μg of pGL3 control plasmid. These complexes were allowed to equilibrate for 30 min at room temperature before adding 42 μl of Tris–HCl buffer or 42 μl of FBS. After 30 min, lipoplexes, lipoplexes plus serum, naked plasmid DNA and naked plasmid DNA plus serum were analyzed by electrophoresis. For this purpose, 10 μl of each sample was mixed with 2 μl of loading buffer (glycerol 30%, bromophenol blue 0.25%) and subjected to agarose gel electrophoresis for 1 h at 80 V. The electrophoresis gel was visualized and digitally photographed using a Kodak Image Station, model 2000 R (Kodak, Rochester, NY).

2.10. Proteomics experiments

All experiments were conducted at least twice to ensure reproducibility of the particle–protein complex pellet sizes, general pattern, and band intensities on the 1D gels. Cationic liposomes and lipoplexes were incubated with different concentrations of human blood plasma in Tris–HCl (10^{-2} M, pH 7.4), NaCl (0.15 M), and EDTA (1 mM). The samples were centrifuged to pellet the particle–protein complexes. The pellet was resuspended in buffer, transferred to a new vial, and centrifuged again to pellet the particle–protein complexes; this procedure was repeated three times. After the third washing step the supernatant did not contain any detectable amount of proteins. The proteins were eluted from the particles by adding SDS-sample buffer to the pellet and boiling the solution. The proteins were separated by 12% SDS/PAGE 1D gels.

3. Results

3.1. Transfection efficiency

Fig. 2 shows the comparison between the transfection efficiency of DC-Chol–DOPE/DNA lipoplexes (white bar) and DC-Chol–DOPE/DNA–FBS lipoplexes (black bar). When in the presence of serum, DC-Chol–DOPE/DNA lipoplexes exhibited a more than 2-fold increase in transfection efficiency. This was a very unusual result because the presence of serum in cell culture medium has frequently been shown to decrease the transfection efficiency of lipoplexes [25,26]. In search of a correlation between transfection behaviour and colloidal stability,

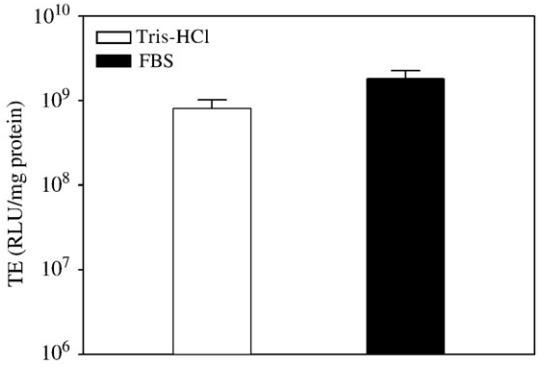

Fig. 2. Transfection efficiency in RLU/mg of cellular proteins of DC-Chol–DOPE/DNA (white bar) and DC-Chol–DOPE/DNA–FBS lipoplexes (black bar).

we have investigated the effect of serum on the structure, size, ζ-potential, and DNA-protection capacity of lipoplexes.

3.2. Synchrotron SAXS

Fig. 3 (top of panel) shows synchrotron SAXS pattern of DC-Chol–DOPE/DNA lipoplexes. X-ray pattern shows sharp Bragg peaks at $q_{001}=0.091$ Å^{-1}, $q_{002}=0.182$ Å^{-1}, $q_{003}=0.273$ Å^{-1}, $q_{005}=0.456$ Å^{-1} (the *004* reflection is absent owing to the form factor, [23]) resulting from the layered structure of the L_α^C phase (Fig. 1) with lamellar *d*-spacing, $d=d_B+d_W=2\pi/q_{001}=68.9$ Å. In addition a broader peak (marked by an arrow) is present. This is usually referred to as 'DNA peak' and it is due to the inter-helical DNA correlation (Fig. 1) with a characteristic spacing, $d_{DNA}=31.8$ Å. Fig. 3 (bottom of panel) shows synchrotron SAXS pattern of DC-Chol–DOPE/DNA–FBS lipoplexes.

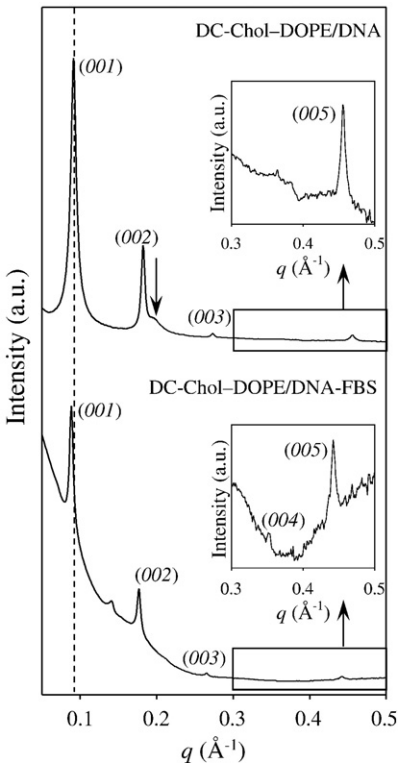

Fig. 3. Representative synchrotron SAXS patterns of DC-Chol–DOPE/DNA and DC-Chol–DOPE/DNA–FBS lipoplexes (from the top to the bottom). Interhelical DNA–DNA distance peak is marked by an arrow. Vertical dashed line identifies the position of the (*001*) Bragg peak of DC-Chol–DOPE/DNA. The insets show a view of the higher-*q* region on an expanded vertical scale.

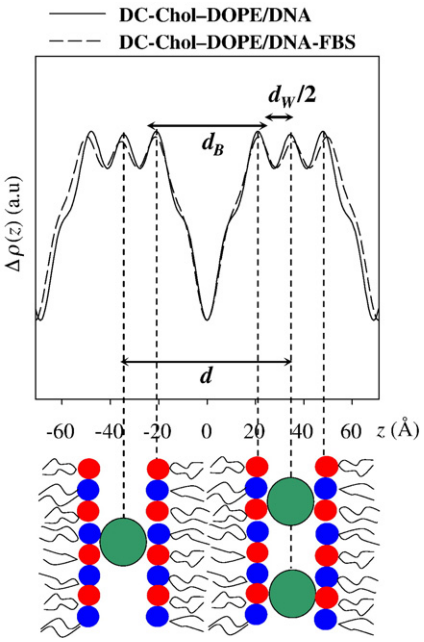

Fig. 4. Electron density profiles along the normal to the bilayers of DC-Chol–DOPE/DNA lipoplexes (continuous line) and DC-Chol–DOPE/DNA–FBS lipoplexes (dashed line). The high-electron-density region, corresponding to the main maxima, reflects the presence of the phospholipid head groups, and the low-electron-density region reflects the hydrocarbon chains. Bilayer parameters are defined: *d*, lamellar repeat distance; d_B, bilayer region thickness; and d_W, interlamellar water layer thickness. Two secondary maxima at the edges of the profile are observed, corresponding to the embedded d_{DNA} molecules.

Sharp peaks were detected at $q_{001}=0.089$ Å^{-1}, $q_{002}=0.177$ Å^{-1}, $q_{003}=0.266$ Å^{-1}, $q_{004}=0.356$ Å^{-1}, $q_{005}=0.443$ Å^{-1} resulting from the L_α^C phase ($d=71.1$ Å). A low-intense peak centred at about $q=0.14$ Å^{-1} was observed. Its origin is not unambiguous. However, the most compelling explanation is that such a scattering contribution arises from pure DC-Chol–DOPE domains formed as a consequence of lipid demixing upon serum proteins binding.

For estimating all relevant structural parameters of lipoplexes, electron density profiles along the normal to lipid bilayers were calculated from the SAXS patterns of Fig. 3. In Fig. 4 comparison between the profiles of DC-Chol–DOPE/DNA (continuous line) and DC-Chol–DOPE/DNA–FBS lipoplexes (dashed line) is presented. The EDPs of Fig. 4 show the usual lipid bilayer density [27–30] plus high-density regions at the outer edges of the profile due to the DNA rod lattices intercalated between opposing bilayers (Fig. 4) [24,31–33]. The electron-denser regions, i.e. the two maxima in the electron density profiles of Fig. 4 depict the headgroups region, while the pronounced central minimum, at $z=0$, corresponds to the terminal methyl groups of the opposing acyl chains. According to recent models [34], the distance between the maxima plus the FWHM of the Gaussian representing polar headgroup provides a reasonable estimate of the membrane thickness, d_B. According to general definitions [34], the lamellar repeat distance *d* is the sum of the membrane thickness, d_B, and the water layer thickness, d_W. Thus, the interbilayer water thickness is usually defined as $d_W=d-d_B$. All calculated structural parameters of DC-Chol–DOPE/DNA lipoplexes and DC-Chol–DOPE/DNA–FBS lipoplexes are listed in Table 1.

Table 1
Lamellar periodicity, *d*, lipid bilayer thickness, d_B, and thickness of the interbilayer water region, d_W, of DC-Chol–DOPE/DNA and DC-Chol–DOPE/DNA–FBS lipoplexes.

	d (Å)	d_B (Å)	d_W (Å)
DC-Chol–DOPE/DNA	68.9 ± 0.1	47.6 ± 0.4	21.3 ± 0.5
DC-Chol–DOPE/DNA–FBS	71.1 ± 0.1	51.5 ± 0.4	19.6 ± 0.5

We observe that the addition of serum to DC-Chol–DOPE/DNA lipoplexes produced two principal outcomes: (i) lamellar structure was conserved with small enlargement of lamellar *d*-spacing (less than 2 Å). Recent studies showed that cationic lipidic vectors recruit large amounts of serum proteins, particularly those containing DOPE as a helper lipid [35]. Thus the observed swelling of DC-Chol–DOPE membranes is due to serum proteins intercalation within lipid bilayers [8,11]. (ii) The DNA peak was not observed in the SAXS pattern. According to recent publications [36,37] the latter finding suggests that DNA packing density was dramatically affected by interaction with serum.

3.3. Size and ζ-potential

Particle size is important for transfection. Since a correlation between structural changes of lipoplexes in FBS and transfection activity could not be detected, we used DLS to investigate the effect of FBS on the size of the DC-Chol–DOPE CLs and DC-Chol–DOPE/DNA lipoplexes. In Table 2 the size of CLs and lipoplexes is reported. In both cases, serum was found to promote a significant increase in particle size by a factor of approximately 3. By simple geometric considerations, it can be inferred that upon interaction with serum, the same number of lipid particles, either CLs or lipoplexes, $N=(D_{FBS}/D_{TRIS})^3 \sim 9$, aggregated. Aside from giving a quantitative description of the serum-induced particle size increase, the similarity between the aggregation behaviour of lipoplexes and free CLs in their interaction with serum seems to prove that the lipid bilayer is the primary target serum proteins interact with.

In Table 2 the ζ-potential for CLs and lipoplexes both in the absence and presence of serum is reported. Such a physical quantity is a widely accepted parameter for physical characterization of particle surface charge. In the absence of serum, ζ-potential of DC-Chol–DOPE/DNA complexes was lower than that of free CLs owing to partial neutralization of the positive charge of cationic lipids by DNA. Following the incubation with serum, the ζ-potential of free CLs reversed to slightly negative (~ −10 mV), while it was definitely more negative in the case of lipoplexes (~ −30 mV).

3.4. Electrophoresis

Serum proteins can promote lipoplex aggregation resulting in DNA release and degradation. To find out whether interaction between serum components and lipoplexes is accompanied by lipid–DNA dissociation, we investigated the extent of DNA release by electrophoresis on agarose gels that allows to determine molar fraction and conformation of the DNA that is completely free from lipid. In Fig. 5, we present the digital photograph of DC-Chol–DOPE/DNA complexes in the absence (lane 1) and presence (lane 2) of FBS. Lane 3 is the control DNA. The high-mobility band was attributed to the most compact (supercoiled) form, whereas the less-intense one was considered to contain the nonsupercoiled content in the plasmid preparation. First, one can observe that no free DNA was observed in lane 1. This finding means that all the plasmid DNA is complexed by DC-Chol–DOPE liposomes. Such a high DNA-binding capacity does correlate with their high transfection efficiency. Indeed, it is well known that DNA-binding ability of liposomes represents a significant barrier to efficient transfection since DNA, when unprotected by a coating of cationic lipid, is subject to rapid degradation by cytosolic DNase [38].

Table 2
Mean diameter, *D*, and ζ-potential, ζ_P, of DC-Chol–DOPE and DC-Chol–DOPE/DNA in the absence and in the presence of FBS.

	D (nm)	ζ_P (mV)
DC-Chol–DOPE	109 ± 2	56.3 ± 1.3
DC-Chol–DOPE–FBS	360 ± 3	−11.4 ± 0.5
DC-Chol–DOPE/DNA	244 ± 4	48.0 ± 1.5
DC-Chol–DOPE/DNA–FBS	741 ± 1	−29.7 ± 0.2

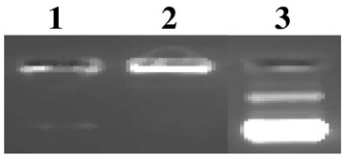

Fig. 5. Digital photograph of DC-Chol–DOPE/DNA lipoplexes (lane 1) and DC-Chol–DOPE/DNA/FBS lipoplexes (lane 2). Lane 3 is the control DNA. The high-mobility band was attributed to the most compact (supercoiled) form, and the less-intense one was considered to be the non-super-coil content in the plasmid preparation.

Noteworthy is that a new band can be seen just below the wells after the incubation with FBS (lane 2). We interpret the new band as plasmid DNA that is released from the lipid surface so that it is available to EtBr, but still confined by cationic–anionic lipid aggregates, so it cannot migrate very far from the wells [39]. Such DNA remains trapped within the confines of the lipid array, but still protected by enzymatic attack. In principles, weakening cationic lipid–DNA interactions may result in a much more efficient DNA release from the confines of the lipid aggregate. Moreover, the presence of serum did not affect the conformation of DNA protected by cationic lipids. Indeed, plasmid DNA extracted from lipoplexes by phenol–chloroform extraction (data not reported) is still present in a supercoiled conformation. Conversely, free DNA was severely affected by serum (data not reported), with topology being shifted to an open-circular conformation. This finding indicates that the serum treatment of DC-Chol–DOPE/DNA lipoplexes did not enhance nuclease accessibility. DNA was therefore completely protected by cationic lipids from nuclease activity.

3.5. Proteomics

Fig. 6 shows SDS-PAGE (12% gels) of plasma proteins retrieved from 0.1 mg of DC-Chol–DOPE and DC-Chol–DOPE/DNA after 45 min of centrifugation (lane B and C, respectively) and 2 min of centrifugation (lane D and E, respectively) and triple washing. The preferred method to separate the nanoparticles from plasma has been centrifugation, but the outcome appears to be the time centrifugation and the duration of washing used in these steps. Sedimentation of large proteins, protein aggregates, and co-precipitation may occur for

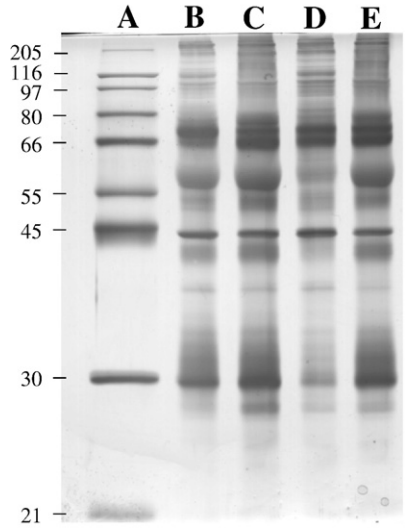

Fig. 6. SDS-PAGE (12% gels) of plasma proteins retrieved from 0.1 mg of DC-Chol–DOPE and DC-Chol–DOPE/DNA after 45 min of centrifugation (lane B and C, respectively) and 2 min of centrifugation (lane C and D, respectively) and triple washing. Lane A is a protein molecular weight markers.

a high centrifugation time. A protein with high abundance in plasma may be associated with the particles because of insufficient washing. Results were not affected by the centrifugation time. Indeed the protein profiles of lanes B and C (45 min of centrifugation) are very similar to those of lanes C and D (2 min of centrifugation). This indicates that, despite three vigorous washes, most proteins remained bound to nanoparticles. Furthermore, the protein profile obtained from DC-Chol–DOPE/DNA (lane C and E) is a bit more intense than that obtained from DC-Chol–DOPE (lane B and D), because most likely the presence of DNA facilitate the protein binding to nanoparticles. A whole range of proteins (perhaps many of them having quite distinct biological roles relevant to nanomedicine and nanosafety) seem to form part of the corona. We show here that these assays are reliable if conducted with care and accompanied by proper control experiments.

4. Discussion

Mechanisms of cationic lipid-based nucleic acid delivery are receiving increasing attention, but despite this the factors that determine high or low activity of lipoplexes under physiological conditions are still poorly understood. We therefore addressed the effect of serum on the transfection efficiency and colloidal stability of the DC-Chol–DOPE/DNA complexes. Since the protein composition of FBS and HP is roughly the same (serum is plasma without clotting factors) and a precise identification of adsorbed proteins goes beyond the scope of the present work, here we have used FBS and HP indifferently. Indeed, previous experiments with serum instead of plasma were made and no differences were observed [40].

In the absence of serum, DC-Chol–DOPE/DNA complexes were found to be fairly efficient (Fig. 2) with respect to the highly efficient commercial Lipofectamine 2000 (Invitrogen) (data not reported). Interestingly, we observed an approximate 2-fold increase in transfection efficiency when lipoplexes were incubated with serum (Fig. 2, black histogram). This was a remarkable result because the presence of serum in cell culture medium has frequently been shown to decrease the transfection efficiency of lipoplexes [25,26]. In search of the physical–chemical factors promoting such an increase in efficiency, we have investigated the effect of serum on the structure, particle size, ζ-potential and DNA-protection capacity.

The structural instability of lipoplexes is one of the possible causes of the low transfection efficiencies usually observed in serum-containing media [41,42]. Our synchrotron SAXS experiments (Fig. 3) showed that the multilamellar arrangement of DC-Chol–DOPE/DNA lipoplexes was maintained in serum. On the other hand, binary mixtures of DOPE and transfection cationic reagents other than DC-Chol did not exhibit the same structural stability. Incorporation of cholesterol or cholesterol-derivatives (such as DC-Chol) in liposome formulations is well known to increase the packing density of phospholipids and reduce permeability to solutes [43]. It has been also reported that the increased packing of phospholipids by cholesterol can prevent their removal by plasma high-density lipoproteins and preserve liposomal stability in the presence of serum [44]. We therefore suggest that the marked stability of DC-Chol–DOPE/DNA lipoplexes, most likely due to the choice of the cationic lipid, is a reasonable explanation of their high efficiency in serum (Fig. 2). On the other hand, DNA packing density was largely affected by interaction with serum components as unambiguously shown by the disappearing of the 'DNA peak' in the SAXS pattern (Fig. 3, bottom panel). These findings support the idea that the multilamellar onion-like structure of lipoplexes (Fig. 1) was not affected by serum, while the inter-DNA correlation vanished. Since formation of the well-ordered 1D DNA lattice within lamellar lipoplexes does depend on polarization of cationic lipids that interact with negatively charged phosphates on the DNA backbone via electrostatic interactions [45,46], the latter finding suggests that, after interaction with serum, DNA is confined within lipoplexes, but the cationic lipid–DNA interaction is lost. Accordingly, the EDP of FBS lipoplexes reported in Fig. 4 (dashed line) shows the increase in electron density at the outer edges of the profile thus confirming the presence of electron-dense DNA between opposing cationic membranes. This interpretation was strongly corroborated by electrophoresis findings showing that a large part of plasmid DNA is released from the lipid surface, but it is still confined by cationic–anionic lipid aggregates (Fig. 5, lane 2).

Among physical–chemical parameters of lipoplexes, size has been reported to be a major determinant of transfection efficiency. Our DLS data (Table 2) show that dimensions of lipoplexes largely increased after interaction with serum. Since the nanostructure of lipoplexes was almost unchanged by serum (Figs. 3 and 4), the most compelling explanation of DLS data is that serum promoted aggregation of intact lipoplexes. Proteomics results were in excellent agreement with such an interpretation since they showed that lipoplexes, after interaction with HP, were covered by a layer of adsorbed proteins (Fig. 6) that are able to promote lipoplex aggregation. Recently, remarkable studies have reported on the existence of a rich protein layer associated with the surface of several copolymer particles after treatment with serum [40,47–49]. However, to the best of our knowledge, our study is the first report in the literature showing the so-called 'protein corona' associated with the surface of lipoplexes after interaction with HP. Proteomics experiments also showed that the electrophoretic patterns of lipoplexes and CLs were roughly the same. Even though an accurate protein quantification and analysis is beyond the scope of the present study, we infer that the surface properties of lipid vesicles are not affected by the DNA. The latter observation is consistent with the model of lipoplex structure reported in Fig. 1 where the DNA is essentially embedded within the multilamellar onion-like structure [5–7]. Remarkably, evidence of such a protein corona associated with the lipid surface most likely suggests that serum proteins acted as a 'molecular glue' in that they forced lipid vesicles, being either CLs or lipoplexes, to come into contact and aggregate by reducing the inter-membrane repulsive barrier essentially due to electrostatic repulsions. Upon charge neutralization, single lipid particles tend to stick when they collide because van der Waals short-range attractions can easily overcome weakened electrostatic repulsions. As a consequence, large aggregates formed (Fig. 7) with lipoplex size increasing from approximately 200 to more than 700 nm (Table 2). Even though the

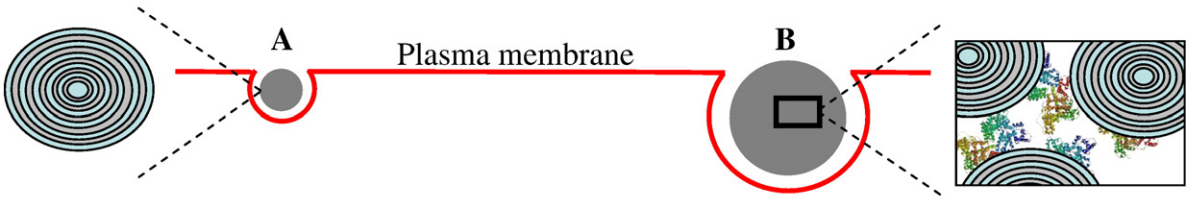

Fig. 7. Schematic presentation of the internalization of lipoplexes (A) and large lipoplex–protein aggregates (B). Adsorbed 'protein corona' (B, inset) promotes formation of large lipoplex aggregated. Finally, depending on their size, lipid nanoparticles either are taken up into the cell via receptor clathrin-mediated (A) or caveolae-mediated (B) endocytosis.

optimal lipoplex size for efficient transfection is currently under debate [16,38], there is general consensus that the most significant role of lipoplex size is (co)determining the nature of the entry pathway of complexes into the cells [16]. There is compelling evidence that endocytosis is the major pathway of lipoplex internalization into cells. However, distinct endocytic pathways exist in eukaryotic cells, with clathrin-dependent and caveolae-mediated internalization being the most relevant ones. Recently, a size-dependent mechanism of lipoplex internalization has been proposed [16,50,51]. Accordingly, lipoplexes with a size approximately of 300 nm or less are supposed to enter cells basically via the clathrin-coated pathway, while complexes larger than 500 nm are internalized via caveolae-mediated pathways. Since the latter pathway seems to avoid lysosomal digestion, complexes larger 500 nm should be able to escape from endosomes efficiently. According to these suggestions, it has recently been claimed that only caveolae-mediated internalization can produce efficient transfection [50]. Consistent with the above-mentioned size-dependent entry mechanism, our data seemingly suggest that the transfection efficiency boost observed in serum (Fig. 2) may be due to a switch from clathrin-dependent to caveolae-mediated internalization induced by the remarkable increase in size promoted by the protein corona associated with the lipid membrane surface.

In search of the reason why DC-Chol–DOPE/DNA lipoplexes exhibit an unusual efficiency increase in serum, it was found that transfection efficiency boost was determined by simultaneous lipoplex stability and increase in size. While the former process is most likely due to the choice of the cationic lipid which help towards packing the phospholipids and reducing membrane permeability to proteins [42,43], the latter is regulated by the adsorption of a protein corona that was found to be associated with the surface of lipoplexes. Such a rich protein layer lowered the interbilayer electrostatic repulsions between cationic lipoplexes thus promoting aggregation of intact complexes. Within the complex, plasmid DNA is no more electrostatically bound to cationic lipids and the 1D DNA ordering is lost. However, plasmid DNA is not released from the complex and maintains its conformation. The increase in size was most likely associated with a switch from a clathrin-dependent to caveolae-mediated internalization resulting in the observed transfection efficiency boost. Controlling size of serum-resistant lipoplex formulations may therefore be a successful strategy to design efficient lipid delivery systems for in vitro and in vivo gene therapy.

Acknowledgments

We acknowledge Dr. T. Narayanan and Dr. E. Di Cola of the experimental staff of ID02 at ESRF for technical support.

References

[1] L. García, M. Buñuales, N. Düzgüneş, C. Tros de Ilarduya, Serum-resistant lipopolyplexes for gene delivery to liver tumour cells, Eur. J. Pharm. Biopharm. 67 (2007) 58–66.
[2] E. Marshall, Gene therapy: what to do when clear success comes with an unclear risk? Science 298 (2002) 510–511.
[3] C. Tros de Ilarduya, M.A. Arangoa, M.J. Moreno-Aliaga, N. Düzgüneş, Enhanced gene delivery in vitro and in vivo by tansferrin-lipoplexes, Biochim. Biophys. Acta 1561 (2002) 209–221.
[4] L.G. De la Torre, R.S. Rosada, A.P. Fávaro Trombone, F.G. Frantz, A.A.M. Coelho-Castelo, C. Lopes Silva, M.H. Andrade Santana, The synergy between structural stability and DNA binding controls the antibody production in EPC/DOTAP/DOPE liposomes and DOTAP/DOPE lipoplexes, Colloids Surf. B: Biointerfaces 73 (2009) 175–184.
[5] I. Koltover, T. Salditt, J.O. Rädler, C.R. Safinya, An inverted hexagonal phase of cationic liposome–DNA complexes related to DNA release and delivery, Science 281 (1998) 78–81.
[6] F. Artzner, R. Zantl, G. Rapp, J.O Rädler, Observation of a rectangular columnar phase in condensed lamellar cationic lipid–DNA complexes, Phys. Rev. Lett. 81 (1998) 5015–5018.
[7] G. Caracciolo, D. Pozzi, R. Caminiti, H. Amenitsch, Multicomponent cationic lipid–DNA complex formation: role of lipid mixing, Langmuir 21 (2005) 11582–11587.
[8] O. Zelphati, L.S. Uyechi, L.G. Barron, F.C. Szoka Jr, Effect of serum components on the physico-chemical properties of cationic lipid/oligonucleotide complexes and on their interactions with cells, Biochim. Biophys. Acta 1390 (1998) 119–133.
[9] S. Li, W.C. Tseng, D.B. Stolz, S.P. Wu, S.C. Watkins, L. Huang, Dynamic changes in the characteristics of cationic lipidic vectors after exposure to mouse serum: implications for intravenous lipofection, Gene Ther. 6 (1999) 585–594.
[10] D. Simberg, S. Weisman, Y. Talmon, A. Faerman, T. Shoshani, Y. Barenholz, The role of organ vascularization and lipoplex-serum initial contact in intravenous murine lipofection, J. Biol. Chem. 278 (2003) 39858–39865.
[11] J.P. Yang, L. Huang, Overcoming the inhibitory effect of serum on lipofection by increasing the charge ratio of cationic liposome to DNA, Gene Ther. 4 (1997) 950–960.
[12] S. Audouy, G. Molema, L. De Leij, D. Hoekstra, Serum as a modulator of lipoplex-mediated gene transfection: dependence of amphiphile, cell type and complex stability, J. Gene Med. 2 (2000) 465–476.
[13] Y. Maitani, S. Igarashi, M. Sato, Y. Hattori, Cationic liposome (DC-Chol/DOPE = 1: 2) and a modified ethanol injection method to prepare liposomes, increased gene expression, Int. J. Pharm. 342 (2007) 33–39.
[14] M. Ramezani, M. Khoshhamdam, A. Dehshari, B. Malaekeh-Nikouei, The influence of size, lipid composition and bilayer fluidity of cationic liposomes on the transfection efficiency of nanolipoplexes, Colloids Surf. B: Biointerfaces 72 (2009) 1–5.
[15] A.R. Price, M.P. Limberis, J.M. Wilson, S.L. Diamond, Pulmonary delivery of adenovirus vector formulated with dexamethasone–sperimine facilitates homologous vector re-administration, Gene Ther. 14 (2007) 1594–1604.
[16] J. Rejman, V. Oberle, I.S. Zuhorn, D. Hoekstra, Size-dependent internalization of particles via the pathways of clathrin- and caveole-mediated endocytosis, Biochem. J. 377 (2004) 159–169.
[17] D. Pozzi, H. Amenitsch, R. Caminiti, G. Caracciolo, How lipid hydration and temperature affect the structure of DC-Chol–DOPE/DNA lipoplexes, Chem. Phys. Lett. 422 (2006) 439–445.
[18] A.J. Lin, N.L. Slack, A. Ahmad, C.X. George, C.E. Samuel, C.R. Safinya, Three-dimensional imaging of lipid gene-carriers: membrane charge density controls universal transfection behavior in lamellar cationic liposome-DNA complexes, Biophys. J. 84 (2003) 3307–3316.
[19] K.K. Ewert, A. Ahmad, H.M. Evans, C.R. Safinya, Cationic-lipid DNA complexes for non-viral gene therapy: relating supramolecular structures to cellular pathways, Expert Opin. Biol. Ther. 5 (2005) 33–53.
[20] N.S. Templeton, Cationic liposomes as in vivo delivery vehicles, Curr. Med. Chem. 10 (2003) 1279–1287.
[21] P. Boesecke, Reduction of two-dimensional small- and wide-angle X-ray scattering data, J. Appl. Cryst. 40 (2007) s423–s427.
[22] V. Luzzati, P. Mariani, H. Delacroix, X-ray crystallography at macromolecular resolution: a solution of the phase problem, Makromol. Chem., Macromol. Symp. 15 (1998) 1–17.
[23] O. Francescangeli, D. Rinaldi, M. Laus, G. Galli, B. Gallot, An X-ray study of a smectic C and smectic A liquid crystal polyacrylate, J. Phys. II France 6 (1996) 77–89.
[24] R. Zantl, L. Baicu, F. Artzner, I. Sprenger, G. Rapp, J.O. Rädler, Thermotropic phase behavior of cationic lipid−DNA complexes compared to binary lipid mixtures, J. Phys. Chem. B 103 (1999) 10300–10310.
[25] L. Vitiello, K. Bockhold, P.B. Joshi, R.G. Worton, Transfection of cultured myoblasts in high serum concentration with DODAC:DOPE liposomes, Gene Ther. 5 (1998) 1306–1313.
[26] J. Turek, C. Dubertret, G. Jaslin, K. Antonakis, D. Scherman, B. Pitard, Formulations which increase the size of lipoplexes prevent serum-associated inhibition of transfection, J. Gene Med. 2 (2000) 32–40.
[27] S. Tristram-Nagle, H. Petrache, J.F. Nagle, Structure and interactions of fully hydrated dioleoylphosphatidylcholine bilayers, Biophys. J. 75 (1998) 917–925.
[28] S. Tristram-Nagle, J.F. Nagle, Lipid bilayers: thermodynamics, structure, fluctuations, and interactions, Chem. Phys. Lip. 127 (2004) 3–14.
[29] Y. Liu, J.F. Nagle, Diffuse scattering provides material parameters and electron density profiles of biomembranes, Phys. Rev. E 69 (2004) 040901.
[30] N. Kučerka, Y. Liu, N. Chu, H.I. Petrache, S. Tristram-Nagle, J.F. Nagle, Structure of fully hydrated fluid phase DMPC and DLPC bilayers using X-ray scattering from oriented multilamellar arrays and from unilamellar vesicles, Biophys. J. 88 (2005) 2626–2637.
[31] G. Caracciolo, D. Pozzi, H. Amentisch, R. Caminiti, One-dimensional thermotropic dilatation area of lipid headgroups within lamellar lipid/DNA complexes, Langmuir 22 (2006) 4267–4273.
[32] G. Caracciolo, D. Pozzi, R. Caminiti, H. Amentisch, Two dimensional lipid mixing entropy regulates the formation of multi-component lipoplexes, J. Phys. Chem. B 110 (2006) 20829–20835.
[33] C. Marchini, M. Montani, A. Amici, H. Amenitsch, D. Pozzi, C. Marianecci, G. Caracciolo, Structural stability and increase in size rationalize the efficiency of lipoplexes in serum, Langmuir 25 (2009) 3013–3021.
[34] G. Pabst, M. Rappolt, H. Amentisch, P. Laggner, Structural information from multilamellar liposomes at full hydration: full q-range fitting with high-quality X-ray data, Phys. ReV. E 62 (2000) 4000–4009.
[35] S. Li, M.A. Rizzo, S. Bhattacharya, L. Huang, Characterization of cationic Lipid–Protamine–DNA (LPD) complexes for intravenous gene delivery, Gene Ther. 5 (1998) 930–937.
[36] G. Caracciolo, D. Pozzi, R. Caminiti, C. Marchini, M. Montani, A. Amici, H. Amenitsch, DNA release from cationic liposome/DNA complexes by anionic lipids, Appl. Phys. Lett. 89 (2006) 233903.
[37] G. Caracciolo, D. Pozzi, R. Caminiti, H. Amenitsch, Interaction of lipoplexes with anionic lipids resulting in DNA release is a two-stage process, Langmuir 23 (2007) 8713–8717.

[38] A. Elouahabi, J.M. Ruysschaert, Formation and intracellular trafficking of lipoplexes and poliplexes, Mol. Ther. 11 (2005) 336–347.
[39] L. Wang, R. Koynova, H. Parikh, R.C. MacDonald, Transfection activity of binary mixtures of cationic O-substituted phosphatidylcholine derivatives: the hydrophobic core strongly modulates physical properties and DNA delivery efficacy, Biophys. J. 91 (2006) 3692–3706.
[40] D. Simberg, A. Weiss, Y. Barenholz, Reversible mode of binding of serum proteins to DOTAP/Cholesterol lipoplexes: a possible explanation for intravenous lipofection efficiency, Hum. Gene Ther. 16 (2005) 1087–1096.
[41] C.Y. Cheung, P.S. Stayton, A.S. Hoffman, Poly(propylacrylic acid)-mediated serum stabilization of cationic lipoplexes, J. Biomater. Sci. 16 (2005) 163–179.
[42] D. Papahadjopoulos, K. Jacobson, S. Nir, T. Isac, Phase transitions in phospholipid vesicles: fluorescence polarization and permeability measurements concerning the effect of temperature and cholesterol, Biochim. Biophys. Acta 311 (1973) 330–348.
[43] T.M. Allen, L.G. Cleland, Serum-induced leakage of liposome contents, Biochim. Biophys. Acta 597 (1980) 418–426.
[44] S. May, A. Ben-Shaul, Modeling of cationic lipid–DNA complexes, Curr. Med. Chem. 11 (2004) 1241–1253.
[45] G. Caracciolo, R. Caminiti, Do DC-Chol/DOPE–DNA complexes really form an inverted hexagonal phase? Chem. Phys. Lett. 411 (2005) 327–332.
[46] T. Cedervall, I. Lynch, M. Foy, T. Berggård, S.C. Donnelly, G. Cagney, S. Linse, K.A. Dawson, Detailed identification of plasma proteins adsorbed on copolymer nanoparticles, Angew. Chem. Int. Ed. 46 (2007) 5754–5756.
[47] T. Cedervall, I. Lynch, S. Lindman, T. Berggård, E. Thulin, H. Nilsson, K.A. Dawson, S. Linse, Understanding the nanoparticle–protein corona using methods to quantify exchange rates and affinities of proteins for nanoparticles, Proc. Natl. Acad. Sci. U. S. A. 104 (2007) 2050–2055.
[48] I. Lynch, T. Cedervall, M. Lundqvist, C. Cabaleiro-Lago, S. Linse, K.A. Dawson, The nanoparticle–protein complex as a biological entity; a complex fluids and surface science challenge for the 21st century, Adv. Coll. Interface Sci. 134–135 (2007) 167–174.
[49] M. Lundqvist, J. Stigler, G. Elia, I. Lynch, T. Cedervall, K.A. Dawson, Nanoparticle size and surface properties determine the protein corona with possible implications for biological impacts, Proc. Natl. Acad. Sci. U. S. A. 105 (2008) 14265–14270.
[50] J. Rejman, M. Conese, D. Hoekstra, Gene transfer by means of lipo- and polyplexes: role of clathrin and caveole-mediated endocytosis, J. Liposome Res. 16 (2006) 237–247.
[51] D. Hoekstra, J. Rejman, L. Wasungu, F. Shi, I. Zuhorn, Gene delivery by cationic lipids: in and out of an endosome, Biochem. Soc. Trans. 35 (2007) 68–71.